

RESEARCH ARTICLE

Time trends, irregularity and multifractal structure on the monthly rainfall regime at Barcelona, NE Spain, years 1786–2019

Xavier Lana¹  | M. Carmen Casas-Castillo²  | Raül Rodríguez-Solà¹  |
Marc Prohom³ | Carina Serra¹ | Maria Dolors Martínez⁴ | Ricard Kirchner²

¹Department of Physics, ETSEIB, Universitat Politècnica de Catalunya-BarcelonaTech, Barcelona, Spain

²Department of Physics, ESEIAAT, Universitat Politècnica de Catalunya-BarcelonaTech, Terrassa, Spain

³Department of Climatology, SMC, Meteorological Service of Catalonia, Barcelona, Spain

⁴Department of Physics, ETSAB, Universitat Politècnica de Catalunya-BarcelonaTech, Barcelona, Spain

Correspondence

Xavier Lana, Department of Physics, ETSEIB, Universitat Politècnica de Catalunya-BarcelonaTech, Diagonal 647, 08028 Barcelona, Spain.
Email: francisco.javier.lana@upc.edu

Funding information

Ministerio de Ciencia, Innovación y Universidades, Grant/Award Numbers: AGL2017-87658-R, PID2019-105976RB-I00

Abstract

A long and complete series of monthly rainfall amounts corresponding to Barcelona city (Catalonia, NE Spain), exceeding two centuries (years 1786–2019), is analysed in detail. The obtained results of periodicity (annual scale), time trends (monthly, seasonal and annual scales), statistical distribution (seasonal and annual scale) and fractal/multifractal structures and self-similarity at monthly scale depict the complex structure of this pluviometric regime, which is characterized by moderate increasing and decreasing trends on rain amounts, varying from $+0.08 \text{ mm}\cdot\text{year}^{-1}$ (February) to $-0.07 \text{ mm}\cdot\text{year}^{-1}$ (September) and quite evident changes on the pluviometric trends at annual and seasonal scales when the rainfall data are analysed for segments of 50 years from 1800 up to 2019. A good example could be the relevant change on the annual scale time trend, from $+0.77 \text{ mm}\cdot\text{year}^{-1}$ (years 1800–1850) to $-0.17 \text{ mm}\cdot\text{year}^{-1}$ (years 1950–2019). Clear evidences of decreasing pluviometry for spring, summer and autumn for the last segment (1950–2019) in comparison with the other three segments, including years 1800–1950, are also detected. Additionally, increasing rainfall patterns complexity, expected difficulties on monthly rainfall forecasting and the increasing irregularity of monthly amounts is also detected by interpreting fractal and multifractal results. Irregularity increases on the monthly rainfall series and on the rainfall regime complexity derived from multifractal parameters, could be associated with the very notable increase of CO_2 emissions into the atmosphere, globally varying from 51.1×10^6 metric tonnes (year 1820) to 36.6×10^9 metric tonnes (year 2019) and the tropospheric concentration increasing from 280.8 ppm (year 1850) to 397.5 ppm (year 2014), being the probable relationship between tropospheric concentrations and changes on rainfall patterns the objective of future researches.

This is an open access article under the terms of the [Creative Commons Attribution-NonCommercial-NoDerivs](https://creativecommons.org/licenses/by-nc-nd/4.0/) License, which permits use and distribution in any medium, provided the original work is properly cited, the use is non-commercial and no modifications or adaptations are made.

© 2022 The Authors. *International Journal of Climatology* published by John Wiley & Sons Ltd on behalf of Royal Meteorological Society.

KEYWORDS

Barcelona metropolitan area, irregularity, monthly rainfall, multifractality, time trends

1 | INTRODUCTION

The pluviometric regimes of Barcelona city, its metropolitan area and Catalonia (NE Spain) have been analysed from different points of view, taking advantage of pluviometric data obtained from the Spanish Agency of Meteorology (AEMET), the Catalan Agency of Meteorology (SMC), the Fabra Observatory of the Royal Academy of Sciences and Arts (RACA, Barcelona) and the urban network of rainfall intensity of the Barcelona city Council (CLABSA-BCASA). Time trends (Lana *et al.*, 2003), extreme values (Lana *et al.*, 2019), characteristics of dry spells (Lana *et al.*, 2001), complexity of the physical mechanism based on multifractal analyses (Lana *et al.*, 2020a), predictability of monthly amounts based on auto-regression algorithms (Lana *et al.*, 2021a), relationships between monthly amounts and atmospheric circulation indexes (Lana *et al.*, 2017) and characteristics of rainfall intensities at the metropolitan area causing floods (Casas *et al.*, 2010; Rodríguez *et al.*, 2013a; 2013b; 2014; Rodríguez-Solà *et al.*, 2017; Casas-Castillo *et al.*, 2018a; Lana *et al.*, 2020b), among others, are some examples. Other strategies and algorithms used in the research of the pluviometric regime patterns are, for instance, Martínez *et al.* (2007) and Burgueño *et al.* (2004, 2005).

A first objective of this research is to improve the accuracy on some results concerning time trends, statistical models and periodicities of the Barcelona city pluviometric regime at monthly, seasonal and annual scales. Another objective is the verification, based on fractal and multifractal analyses along two centuries, of the complexity degree of the physical mechanism governing the rainfall regime. Additionally, the probable effects of the climatic change on statistically significant time trends and irregularity of the rainfall series are analysed. Expected reduction of rainfall amounts at monthly or annual scale, accompanied by an increase of extreme and short intensity episodes in the Mediterranean basin (Pérez and Boscolo, 2010; Miranda *et al.*, 2011), suggest increases on the irregularity on monthly, seasonal and annual amounts. Nevertheless, other analyses of pluviometric regimes in the Mediterranean (Liuzzo and Freni, 2015) have detected both positive and negative significant time trends on heavy rainfall episodes. From the global viewpoint, the behaviour of the pluviometric regime affected by the climate change varies depending on the geographic emplacement. An example could be that corresponding to Scotland (United Kingdom), where

increases in river flows in four catchments in the West of Scotland were detected (Mansell, 1997), suggesting a possible increase on rainfall amount. Another example could be East Java, Indonesia, where negative trends on accumulated rainfall were detected (Aldrian and Djamil, 2007), or Alabama where less intense IDF curves for short events were observed (Mirhosseini *et al.*, 2013). Redesign of drainage on metropolitan areas (Arnbjerg-Nielsen *et al.*, 2013) should be also considered due to possible increases of very intense short episodes generated by the climate change. Bearing in mind all these examples and an assumed not negligible influence of climate change on rainfall regimes, the long pluviometric record of Barcelona city, covering more than two centuries, is analysed in detail.

Section 2 describes the way how the sequence of monthly amounts was obtained and introduces the first basic results concerning the annual amount records. Section 3 includes a summary of concepts, associated with mathematical theory and algorithms, permitting to determine the complexity and uncertainties concerning the pluviometric regime at monthly scale. The process to quantify the irregularity of the rainfall series, based on self-similarity theory, is introduced in section 4. A summary of the results concerning analyses of fractality, multifractality, time trends significance, statistical models, spectral analysis and irregularity are described in section 5. The obtained results are evaluated in section 6, where a better relationship between CO₂ concentration and changes on rainfall time trends, fractal irregularity and fractal complexity, are assumed for future researches. Finally, section 7 summarizes the most relevant results obtained and causes of time trend and multifractal complexity changes, as well as rainfall irregularity increases, all of them probably related to the increasing quantity of CO₂ in the troposphere, which could be a relevant question to be accurately analysed in future researches.

2 | DATABASE

Bearing in mind that the notably long and complete rainfall series in Barcelona city corresponds to the Fabra Observatory records (1917–2020), this data set could be used for all the summarized objectives in the introduction of this paper. Nevertheless, a detailed research of climatologists, physicists, geographers and historians, taking advantage of useful techniques, algorithms and

pluviometric data, published a few years ago (Prohom *et al.*, 2015) a reconstruction of the monthly pluviometric series in Barcelona city (years 1768–2019) including, among others, the Fabra Observatory data, the longest and complete record. The first rainfall records (1786–1913) were recorded by different consecutive rain gauges within Barcelona city, with emplacements distanced as much as 150 m and a range from 6 to 23 m a.s.l. Since year 1914 up to nowadays, rainfall records were obtained from Fabra Observatory (Reial Acadèmia de Ciències i Arts) at 412 m a.s.l. and approximately at 4.4 km towards the NW of the previous emplacements (years 1786–1913). The quality control and data homogenization were achieved by means of the HOMER method (Prohom *et al.*, 2015), being detected outlier data (exceeding five times interquartile data), as well as distinguishing zero monthly amounts (not rare in Mediterranean areas) and lack of data (15 lost monthly values since 1844–1854). This quality control was also applied taking advantage of available data corresponding to the MSC (Meteorologic Service of Catalonia), AEMET (Spanish Agency of Meteorology), Western Mediterranean (South of France) and Northern Italy records, being considered, by means of the Pearson coefficient, the degree of correlation within the different monthly rainfall series and the set of Barcelona city and Fabra observatory data. A more detailed description of all this process of homogenization and validation of monthly data, the longest pluviometric record of the Iberian Peninsula and one of the longest European rainfall series, is found in Prohom *et al.* (2015). Additionally, annual rainfall amount quality data recorded at the Fabra Observatory (years 1914–2020) has been recently verified by Martín-Vide and Moreno-García (2021). Similar processes have permitted to obtain other long historical record lengths in Europe, being a good example one of the longest monthly record since 1711 to 2016 (Murphy *et al.*, 2018) in Ireland, coinciding with a notable part of the Little Ice Age, the end of this climatic episode, and the increasing continuity of the temperatures along the 20th and 21st century (Mann, 2003). Two examples in the Iberian Peninsula of notable long recordings are, for instance, that of the San Fernando Observatory (Cádiz, Southern Spain; Estévez *et al.*, 2022) and the Astronomic Observatory (Madrid, Central Spain), since years 1805 and 1854 up to nowadays, respectively.

A first basic description of the pluviometric regime is shown in Figure 1, with the annual evolution of the rainfall amounts, characterized by an average annual amount of 596.2 mm, a standard deviation of 153.3 mm and close to 25% of annual amounts out of the average \pm standard deviation interval. In agreement with these data, the pluviometric regime would be characteristic of Mediterranean areas (low average, notable standard deviation and

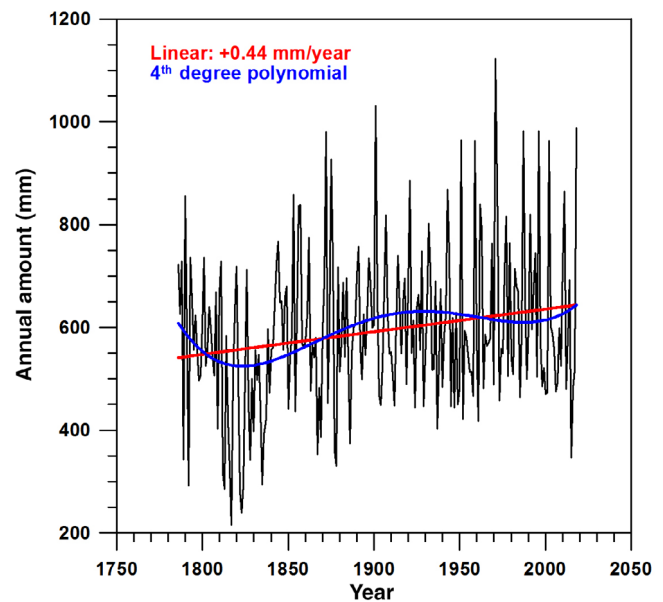


FIGURE 1 Annual evolution of rainfall amounts (1786–2019). The straight and curved lines drawn across the annual register correspond, respectively, to linear and fourth degree polynomial trends [Colour figure can be viewed at wileyonlinelibrary.com]

annual irregularity). Besides a statistically significant (90%) time trend ($+0.44 \text{ mm}\cdot\text{year}^{-1}$) detected in the annual record for years 1786–2019, the mentioned irregularities seem to increase with time by observing that a no negligible increasing number of annual amounts exceed 900 mm after 1850. The detected annual time trend could contribute to these more usual amounts exceeding 900 mm. Nevertheless, the quantified $+0.44 \text{ mm}\cdot\text{year}^{-1}$ should not be the unique consequence of these irregularities, and a more detailed analysis of the irregularity at annual, seasonal and monthly scales is one of the objectives of this manuscript.

The CO_2 global emissions and tropospheric concentration data have been obtained from the websites <https://www.statista.com> and www.co2.earth, and from Meinshausen *et al.* (2017). Meinshausen *et al.* (2017) provided a long-term data sets that constitutes a plausible reconstruction of historical atmospheric concentrations of 43 greenhouse gases (GHGs) to be used in the Climate Model Intercomparison Project Phase 6 (CMIP6) experiments. They focused on the period 1850–2014 for historical CMIP6 but data were also provided for the last 2,000 years. In contrast to previous intercomparisons, the data sets are latitudinally resolved and include seasonality. This data set are based on observations from the worldwide network of NOAA and AGAGE stations and provided records for the pre-observational time from measurements of archived air as well as Antarctic and Greenland ice core and firn data over the last 2,000 years.

3 | FRACTAL AND MULTIFRACTAL THEORY

3.1 | Reconstruction theorem

Several aspects concerning randomness or persistence, complexity, loss of memory and degree of complexity of the physics mechanisms governing rainfall amounts at monthly scale can be analysed by means of the fractal theory, based on the reconstruction theorem (Grassberger and Procaccia, 1983a; Diks, 1999), and the multifractal spectrum algorithm (Kaplan and Yorke, 1979; Grassberger and Procaccia, 1983b; Kantelhardt *et al.*, 2002). Some examples, among many others, of these analyses applied to climatological variables are those corresponding to the thermometric regime (Burgueño *et al.*, 2014) and the monthly rainfall amount (Lana *et al.*, 2020a; 2021b) in Catalonia, NE Spain.

The reconstruction theorem (Diks, 1999) permits to quantify, in terms of the Hurst exponent, H , the degree of randomness, persistence or antipersistence of time series (Korvin, 1992). The same theorem, taking advantage of the correlation integral definition (Grassberger and Procaccia, 1983a, 1983b), quantifies the degree of complexity (increasing with the embedding dimension, μ , exponent) and the loss of memory of the physics system (Kolmogorov exponent, κ). Additionally, the uncertainty degree on the predictability of the time series is quantified by means of the Lyapunov exponents, λ_i (Kaplan and Yorke, 1979; Wiggins, 2003), which can be computed according to the algorithms proposed by Eckmann *et al.* (1986) and Stopp and Meier (1988). All these fractal parameters permit to analyse the degree of complexity of physics mechanisms, as well as quantify the uncertainties on the forecasting of the variables describing it.

3.2 | Multifractal spectrum

Nature phenomena are sometimes not sufficiently described by means of the theory and exponents introduced in the previous paragraph. Many times, the physics mechanisms governing nature phenomena are nonlinear and very complex, being convenient the complementary analyses of their multifractal structures. Besides analyses applied to climatic data (rainfall and thermometric regimes for instance), the seismology is another example of complex field on Earth sciences (Goltz, 1997; Turcotte, 1997) and several authors have also applied the multifractal theory to time series and spatial data. Time series describing these complex mechanisms can be analysed by applying the specific multifractal detrended

fluctuation algorithm (MDFa) (Kantelhardt *et al.*, 2002) being then obtained the multifractal spectrum and the corresponding parameters: the central, maximum and minimum Hölder exponents, α_0 , α_{\max} , α_{\min} , the spectral amplitude, $W = \alpha_{\max} - \alpha_{\min}$, the multifractal asymmetry, $\gamma = (\alpha_{\max} - \alpha_0)/(\alpha_0 - \alpha_{\min})$, the generalized Hurst exponent (being a particular case the Hurst exponent introduced at the beginning of this section) and the complexity index, CI, proposed by Shimizu *et al.* (2002) which is based on parameters α_0 , W and γ , and summarizes the complexity degree of the analysed series. In agreement with the concepts of “physics mechanisms complexity degree,” high values of central Hölder exponents, high spectral multifractal amplitudes and asymmetries notably exceeding 1.0 will represent relevant complexity. Conversely, spectral amplitudes close to zero ($\alpha_{\max} \approx \alpha_{\min}$) suggest monofractal structures with minimum complexity. All these mentioned multifractal parameters, based on the Hölder exponent concept, can be obtained assuming that empiric multifractal spectra are analytically described by the second order polynomial

$$F(\alpha) = C + B(\alpha - \alpha_0) + A(\alpha - \alpha_0)^2, \quad (1)$$

accomplishing $F(\alpha_{\max}) = F(\alpha_{\min}) = 0$ and $F(\alpha_0) = 1$.

A more detailed explanation of the mathematical formulation concerning fractal and multifractal analyses can be found, for instance, in Lana *et al.* (2020a).

4 | SELF-SIMILARITY SCALING

Besides the reconstruction theorem and the multifractal analysis, another monofractal analyses has been widely used in precipitation and hydrological research along the last few decades (Gupta and Waymire, 1990; Koutsoyannis and Foufoula-Georgiou, 1993; Burlando and Rosso, 1996; Menabde *et al.*, 1999; Nhat *et al.*, 2007; Bara *et al.*, 2010; Rodríguez-Solà *et al.*, 2017; Casas-Castillo *et al.*, 2018a; 2022), contributing to quantify the evolution of the time series irregularity, and a good interpretation of fractal scaling also would be found in the research of Zhang *et al.* (2017). As other natural phenomena looking statistically the same regardless of the temporal scale of observation, rainfall often exhibits self-similarity, with some properties accomplishing power laws of a scale parameter λ which is the ratio between any two temporal scales. For instance, it is well known that the annual maximum rainfall intensity series fulfil scale relationships, and then it is possible to relate the probability distribution of the annual maximum intensity I_t for any duration t to the distribution at other temporal scale λt using a factor that is a power function of λ . The equality

between two probability distributions given by Equation (2)

$$I_t = \lambda^\beta I_{\lambda t} \quad (2)$$

is usually referred as “simple scaling in the strict sense” (Gupta and Waymire, 1990; Yu *et al.*, 2004) and implies that all the statistical features of both distributions, including the moments and quantiles, accomplish the equality, being β a scaling parameter.

The Equation (3)

$$\langle I_t^q \rangle = \lambda^{\beta q} \langle I_{\lambda t}^q \rangle \quad (3)$$

expresses the scaling relationship of the statistical moments of order q of the rainfall intensity for a duration t , $\langle I_t^q \rangle$, where the exponent βq can be considered as the linear case of a general scaling function $K(q)$, which is a nonlinear function in the multifractal case (Rodríguez *et al.*, 2013a).

The value of the scaling parameter β has been observed in accordance with the rainfall characteristics of the place of study, especially rain irregularity (Rodríguez-Solà *et al.*, 2017; Casas-Castillo *et al.*, 2018a; 2018b; 2022). The simplest procedure to determine this parameter is to calculate the statistical moments of the maximum annual series for a given duration t (for instance, daily amounts) and the moments of the maximum annual series for several durations λt obtained by aggregation (for instance, rainfall amounts for 2, 3, 4... consecutive days). Then, straight lines obtained by linear regression between the logarithmic values of those moments for every value of q indicate scale invariance within the scaling regime, being βq the value of every slope. Because of its definition, the values of the scale parameter must be greater than -1 , which is a limit value corresponding to a rainfall sample with isolated annual maxima. That is, in the case of daily rainfall, a maximum value of P_1 for a specific day surrounded by dry days. The aggregation process gives rise then to series for which the precipitation for n days, P_n , is the same as P_1 . In terms of the intensity of precipitation this would imply that $I_n = I_1/n$, which compared to the scaling relationship $I_1/n = n^\beta I_1$ for the mean ($q=1$) corresponds to the case $\beta = -1$. The hypothetical opposite case would be that of a totally regular sample for which every day is raining the same, so $P_n = nP_1$ and $I_n = I_1$, that is, the same intensity for all durations, and therefore $\beta = 0$. For real daily rainfall this parameter generally oscillates between values close to -1 and to -0.5 (Rodríguez-Solà *et al.*, 2017; Casas-Castillo *et al.*, 2018a; 2018b; 2022).

The monofractal hypothesis is usually valid only for a limited scaling regime and out of this range the scaling exponent β could change. Many rainfall scaling studies

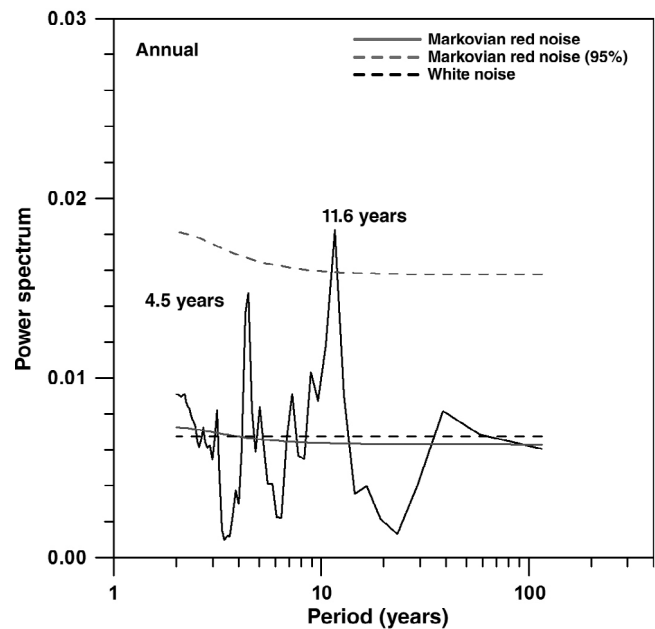


FIGURE 2 Power spectrum for annual amounts

reported a scaling temporal break when the considered duration achieves a value between 1 and 3 weeks, possibly related to the usual lifetime of the major synoptic scale events (Fraedrich and Larnder, 1993; Ladoy *et al.*, 1993; Olsson, 1995; Tessier *et al.*, 1996; De Lima and Grasman, 1999; Royer *et al.*, 2008; De Lima and De Lima, 2009; García-Marín *et al.*, 2013; Rodríguez *et al.*, 2013a; 2013b). For Barcelona (Catalonia, Spain), Rodríguez *et al.* (2013a) and Rodríguez-Solà *et al.* (2017) obtained a scaling regime with an upper limit of the scaling range of 22 days, showing discrepancies for durations below 1 hr, explained in part by the resolution of the measuring instrument. Rodríguez-Solà *et al.* (2017) found for the city of Barcelona a value of the parameter β of -0.78 , both from the digitalized records of a Jardí intensity pluviograph of the Fabra Observatory of Barcelona and from the simultaneous daily record of a totalizer Hellmann gauge located in the same observatory. The Jardí intensity pluviograph, a very innovative device at the time it was invented (1921), gets the diagram of the rainfall intensity over time on strip charts, later digitalized, with a response time of about 10 s. One of the first Jardí gauges was installed in the Fabra Observatory of Barcelona, where it has been operating since 1927 up to the present (Burgueño *et al.*, 1994; Casas *et al.*, 2004). The single scaling regime found for the records from both devices by Rodríguez-Solà *et al.* (2017) ranged from 20 min to 20 days. In the present work, due to the use of monthly data, a different scaling regime in the range of months is expected to find.

5 | RESULTS

The available long series of monthly rainfall amounts in Barcelona is basically characterized by a periodicity of 11.6 years, close to that corresponding to the predominant solar activity (Cameron and Schüssler, 2019) and

another of 4.5 years (Figure 2). Whereas for the spectral peak of 11.6 years the power spectral amplitude overpass white-noise and 95% Markovian red-noise probability, the other relevant periodicity of 4.5 years is characterized by a power spectra only exceeding the white-noise but not the 95% level of Markovian red-noise. It is also worth

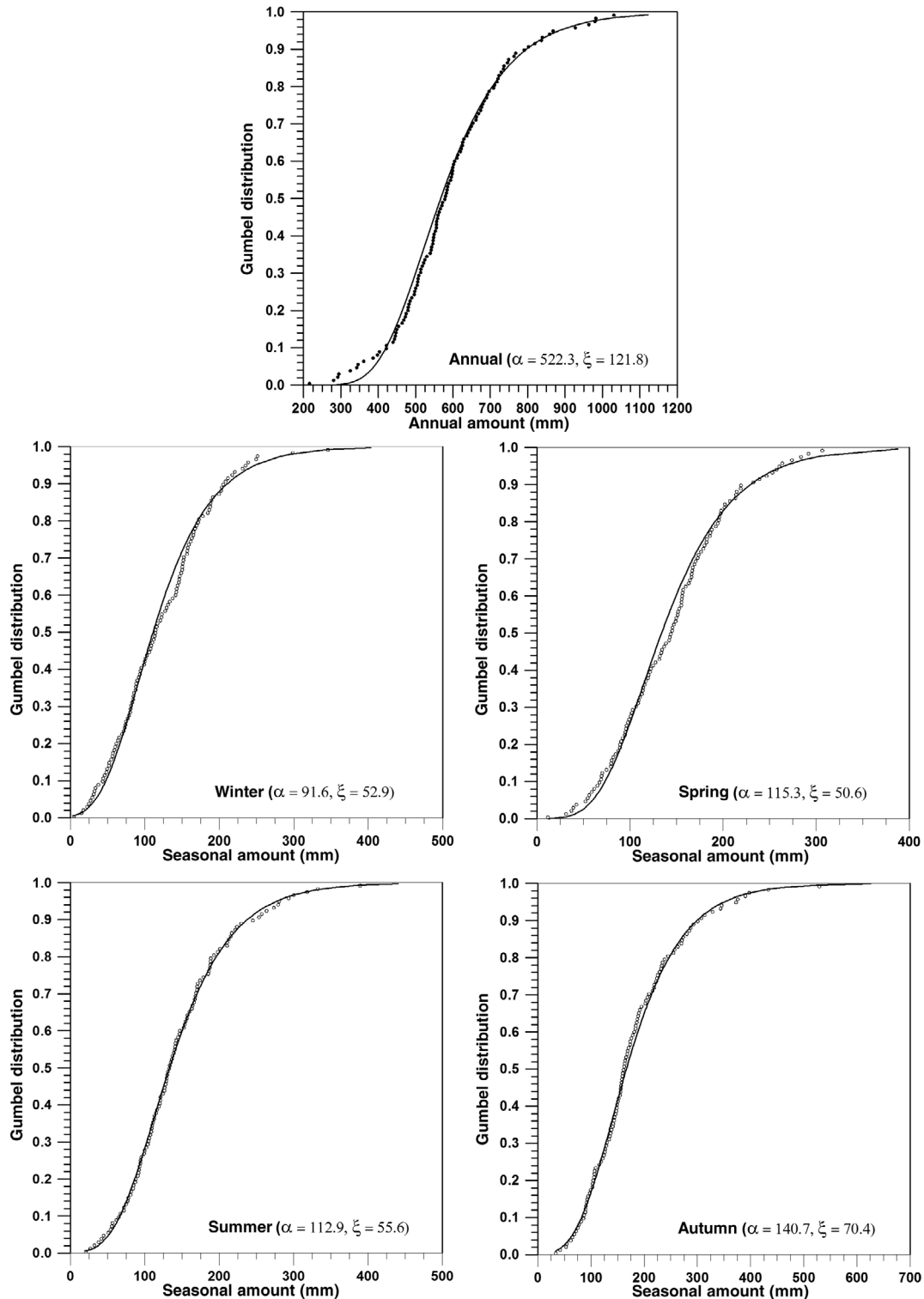


FIGURE 3 Empirical statistical distribution and Gumbel distribution model (solid line) for the annual and seasonal amounts

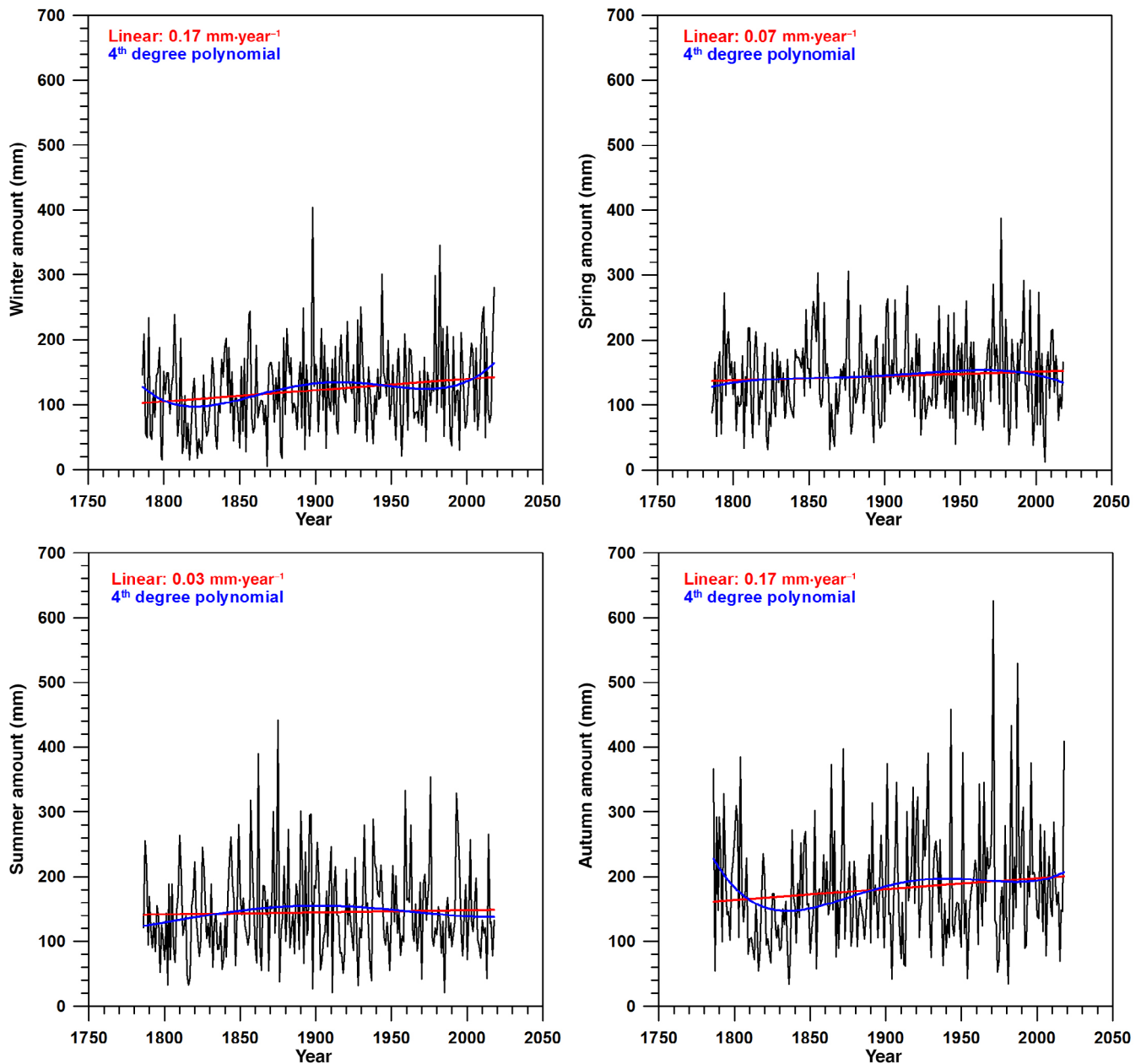


FIGURE 4 Seasonal evolution of rainfall amounts (1786–2019). The straight and curved lines drawn across the seasonal registers correspond, respectively, to linear and fourth degree polynomial trends [Colour figure can be viewed at wileyonlinelibrary.com]

mentioning (Figure 3) that the empiric statistical distribution of seasonal and annual amounts fit well the same cumulated distribution function, the Gumbel model, mathematically represented by

$$F(x) = e^{-e^x}; x = \frac{r - \xi}{\alpha}; -\infty < x < \infty, \quad (4)$$

with parameters (α, ξ) determined with the L -moments formulation (Hosking and Wallis, 1997). This model has been chosen by comparing Euclidean distances between empiric L -skewness and L -kurtosis and those

corresponding to a variety of statistic theoretical models. In spite of this chosen model is usually appropriate to analyse extreme episodes, the results of the L -moments theory proofs that in this case the best fit for the four seasons is offered by the Gumbel distribution, after checking 12 commonly used theoretical distributions. It is also worth mentioning that the best fit to the Gumbel model is achieved for summer and autumn seasons, being also small the discrepancies detected in winter and spring seasons. At annual scale the discrepancies between empiric and theoretical distribution functions for the 200–550 $\text{mm}\cdot\text{year}^{-1}$ range (Figure 3) are a bit more relevant,

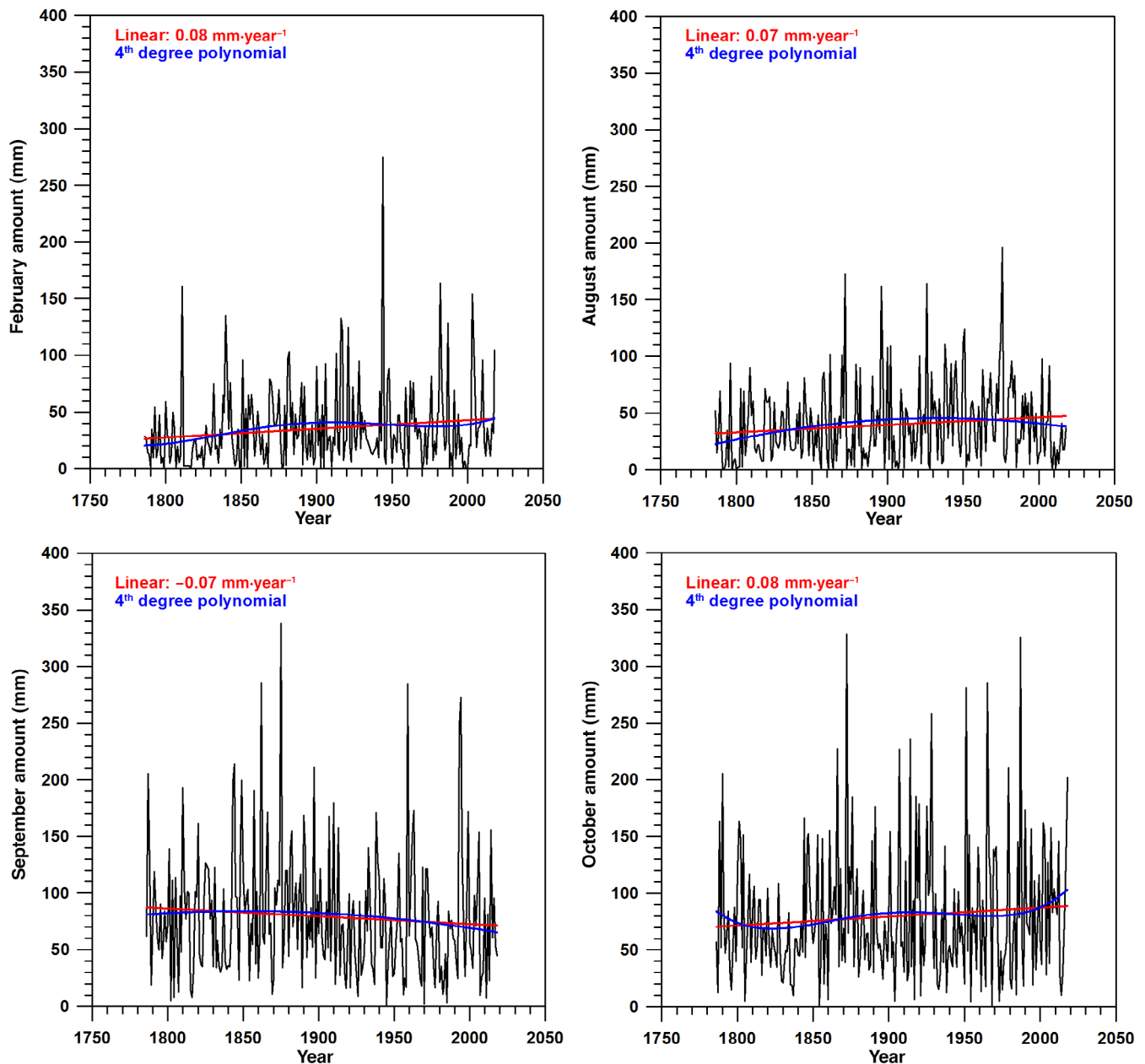


FIGURE 5 Monthly evolution of rainfall amounts (1786–2019) for months with the most outstanding time trends interval (-0.07 to $+0.08$ $\text{mm}\cdot\text{year}^{-1}$). The straight and curved lines drawn across the monthly registers correspond, respectively, to linear and fourth degree polynomial trends [Colour figure can be viewed at wileyonlinelibrary.com]

being then assumed that the Gumbel model is not the most appropriate function in this case. This question should not be a great problem, given that the proved quality of the pluviometric data permits, if it was necessary, to substitute theoretical probability of annual rainfall amounts by the empiric values.

Another relevant question is the statistically significant time trends detected at annual (Figure 1) and seasonal scale (Figure 4), considering the whole (1786–2019) years interval. Time trends have been analysed assuming linear and fourth order polynomial functions and their statistical significances have been quantified by means of

the Mann–Kendall test. All the four seasons and annual data are characterized by moderate positive trends, being detected trends exceeding 95% statistical significance for winter season and 90% for autumn and annual data. The most significant cases at monthly scale are shown in Figure 5, with February, August and October without exceeding positive 0.08 $\text{mm}\cdot\text{year}^{-1}$ trends and September with a negative trend of -0.07 $\text{mm}\cdot\text{year}^{-1}$. Table 1 summarizes all time trends and their statistical significance, with bold types representing cases equalling to or exceeding 90% of statistical significance, for the 1786–2019 years interval. Despite the detected time trends, statistically

TABLE 1 Mann–Kendall percentage of statistical significance of the time trend and increasing or decreasing trend, given in $\text{mm}\cdot\text{year}^{-1}$, for the (1786–2019) interval

	MK%	$\text{mm}\cdot\text{year}^{-1}$
January	10	0.04
February	95	0.08
March	80	0.05
April	45	0.03
May	70	0.05
June	10	0.01
July	45	0.03
August	90	0.07
September	90	−0.07
October	55	0.08
November	5	0.04
December	65	0.05
Annual	90	0.44
Winter	95	0.17
Spring	65	0.07
Summer	35	0.03
Autumn	90	0.17

Note: Bold types correspond to time trends assumed statistically significant ($\geq 90\%$).

significant or not, are characterized by very small amounts (monthly amounts less than $0.1 \text{ mm}\cdot\text{year}^{-1}$ and annual amounts achieving $0.44 \text{ mm}\cdot\text{year}^{-1}$), it has to be remembered that these trends have been estimated bearing in mind monthly records exceeding two centuries, and the cumulate changes on recorded rainfall amounts since 1786 up to the present are not negligible. The time trends at seasonal and annual scale for (1900–1950) and the last 70 years (1950–2019) are quite different. Excepting winter, the annual and the other three seasonal series depict negative time trends (Table 2), being noticeable some of them. Consequently, the differences between the whole recorded years and the 1900–2019 years interval are quite notable, being assumed statistically significant trends (90% level) as those written in bold types.

The complexity of a physics mechanism, in this case that governing the rainfall patterns, can be quantified from the viewpoint of the fractal and multifractal structure of the monthly amount records. Bearing in mind that 2,800 consecutive monthly amounts are available, this high number permits a global fractal and multifractal analysis of the complete data series, as well as an additional multifractal analyses applied to consecutive sets of monthly data delimited by moving windows of 50 years with shifts of 5 years.

TABLE 2 Increasing and decreasing trends at annual and seasonal scales ($\text{mm}\cdot\text{year}^{-1}$) for (1800–1850), (1850–1900), (1900–1950) and (1950–2019) years interval

	1800–1850	1850–1900	1900–1950	1950–2019
Annual	+0.77	+0.10	−1.39	−0.17
Winter	−0.13	+0.79	+0.17	+0.51
Spring	+0.75	−1.04	−0.65	−0.30
Summer	+0.77	+0.38	−0.04	−0.42
Autumn	−0.62	−0.02	−0.73	−0.05

Note: Bold types describe trends exceeding 90% of significance in agreement with the Mann–Kendall test.

From the point of view of the reconstruction theorem, the complexity of the complete monthly rainfall series could be quantified by means of the Hurst exponent. Nevertheless, the value of this exponent is finally deduced from the viewpoint of the multifractality and the generalized Hurst exponent. Another point of view of the complexity, based on fractal theory and reconstruction theorem, is the correlation integral, $C(r)$. Every slope, or embedding dimension $\mu(m)$, of the different $[\log\{C(r)\} - r]$ curves (Figure 6a) for different reconstruction dimensions m quantifies the necessary number of nonlinear equations to describe the physical process. The evolution of this parameter μ^* tends asymptotically (Figure 6b) to the optimum number, d_E , of nonlinear equations to describe the physics mechanism. At the present case, 10 nonlinear equations would be the minimum number to study the physics mechanism of the monthly pluviometric regime in Barcelona. Another relevant point of view is the “loss of memory” of the physical process, manifested by the Kolmogorov entropy and represented by the κ exponent. Details concerning a right determination of this exponent can be found in Lana *et al.* (2020a) and they are summarized in Figure 6c. The deduced value of $\kappa = 1.75$ suggests that autoregressive algorithms to predict with accuracy forthcoming monthly amounts would need a notable number of previous monthly amounts (the optimum case with a minimum number would be for κ close to zero). Additionally, the numerical uncertainties on the monthly forecasting would be conditioned by the Lyapunov exponents, especially the first exponent λ_1 , given that high Lyapunov values could imply notable numerical uncertainties on the forthcoming monthly amount. Figure 6d describes the evolution of the three first Lyapunov exponents, after close to 1,800 iterations to obtain them with a good level of accuracy.

The MDFA multifractal algorithm applied to the whole set of monthly data, offering a global vision of the multifractal structure of the monthly rainfall in Barcelona, is characterized by the following parameters.

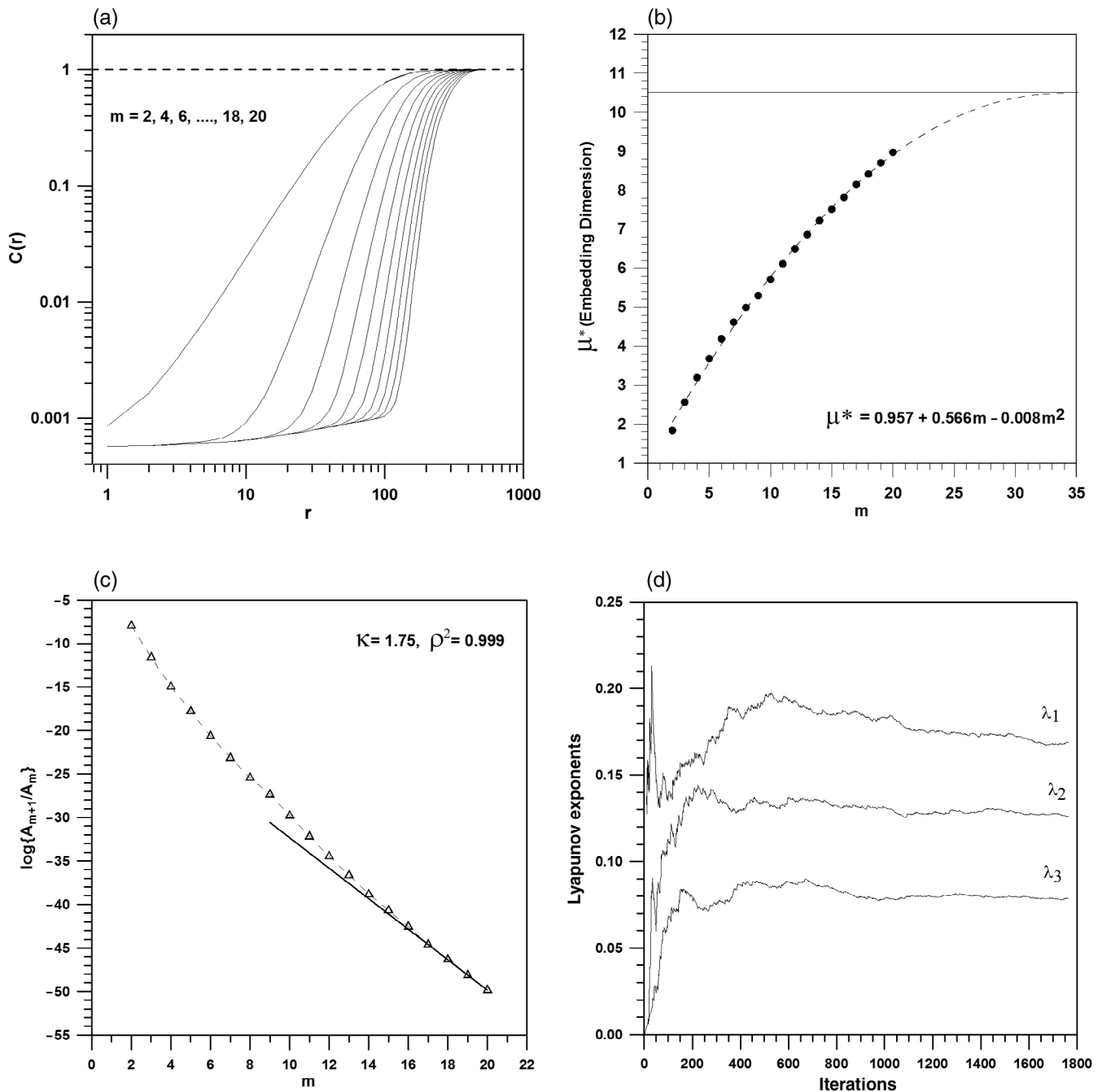


FIGURE 6 Fractal parameters, based on the reconstruction theorem, of the monthly rain amounts: (a) correlation integral, (b) embedding dimension, (c) Kolmogorov entropy, (d) the three first Lyapunov exponents

In agreement with the generalized Hurst exponent curve (Figure 7a), the Hurst exponent $H(q = 2)$ value of 0.43 can be immediately deduced. Instead of persistence or randomness, the monthly rainfall would be characterized by antipersistence close to randomness. The second-order polynomial (Equation (1) and Figure 7b) represents the multifractal spectrum and manifests a notable spectral amplitude (W slightly exceeding 0.9), a central Hölder exponent α_0 close to 4.5, and asymmetry with $(\alpha_{\max} - \alpha_0)$ greater $(\alpha_0 - \alpha_{\min})$. These three parameters are relevant,

as they define the complexity index (CI) of the associated physics mechanisms.

More detailed information concerning the monthly series and, especially, the time evolution of the multifractal parameters can be achieved by means of the mentioned before moving window process. Figure 8a depicts the evolution of the central Hölder exponent, α_0 , for the different moving windows of 50 years length and shift of 5 years for every step. The fluctuations are quite evident, but the linear trend does not suggest notable changes

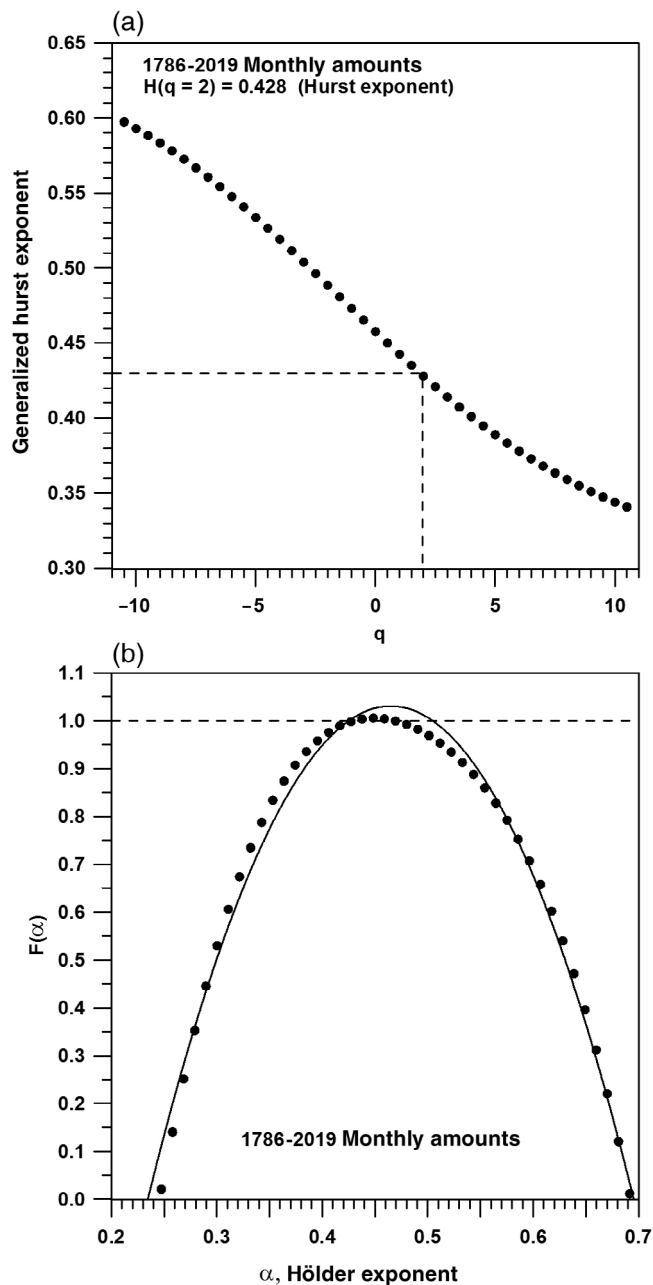


FIGURE 7 (a) Generalized Hurst exponent and (b) multifractal spectrum for the whole monthly amounts dataset

since the end of the 19th century until the beginning of the 21st century. Nevertheless, the maximum Hölder exponent, α_{\max} , and the spectral amplitude, W , show clear increasing tendencies (Figure 8b,c) of 0.010 and 0.012 years^{-1} , respectively. Taking into account that the spectral amplitude is a factor included in the CI, the complexity of the multifractal structure is expected to increase along 19th, 20th and 21st centuries. The evolution of the asymmetry (Figure 8d) does not show relevant tendencies, with γ close to 1.0 (complete symmetry), excepting for two peaks in the 18th century and at the

beginning of the 21st century. As a summary of all these factors, Figure 8e depicts the evolution of the complexity index, with a clear increasing trend of 0.10 years^{-1} and clear increments since, approximately, year 1950. Nevertheless, the oscillations are notable and after the beginning of the 21st century CI approaches to zero, which would be a situation of moderate complexity. Finally, Figure 8f shows the evolution of the Hurst exponent, H ($q = 2$), being remarkable the oscillations from persistence to randomness and anti-persistence, but without a clear time trend along the two centuries. Nevertheless, a reduction on the oscillation amplitude is observed. In agreement with this detail, the series of future monthly amounts would tend in the future to be more randomness than persistent or antipersistent.

After considering the increasing spectral amplitude, it is quite evident that the series of monthly amounts depict multifractal structure along the whole recording period, given that W is notably different from zero. This multifractality character is compatible with the self-similarity structure of rainfall amounts, which permits to quantify the irregularity degree of monthly amounts. In agreement with section 4, Figure 9a shows a log-log representation of the q -order statistical moments of the annual maximum amounts obtained by aggregation of the rainfall monthly data of Barcelona (years 1840–2019), together with linear regressions for every order q of the moments, with scale invariance ranging from 1 to 9 months. Figure 9b depicts the slopes of each line detected in Figure 9a, conforming the linear scaling function $K(q) = \beta q$, with a value of β (-0.50), lower than the scaling parameter found from daily records (Rodríguez-Solà *et al.*, 2017). This is an expected result since a coarser aggregation leads to a smooth sample and monthly series are more regular than daily ones.

Taking the scaling parameter β as an indicator of rainfall irregularity, variations of its value for a long sample, in accordance to possible timed changes, are usually detected. Several studies reported a decreasing dominant trend due to climate change of the annual precipitation in the Mediterranean area in the last recent decades (Pérez and Boscolo, 2010), while an increase of extreme precipitation is expected, related to a greater occurrence of shorter and more intense rainy events (Christensen and Christensen, 2003). In accordance to this, Rodríguez *et al.* (2014) obtained a decrease of the annual precipitation of Barcelona of at least 5% during the last third of the 21st century, whereas a future increase of the extreme daily rainfall was estimated. Furthermore, the expected increase was slightly higher for the hourly rainfall amounts compared to daily ones. To detect changes in the scaling behaviour of rainfall series according to the reported decreasing trend in annual precipitation

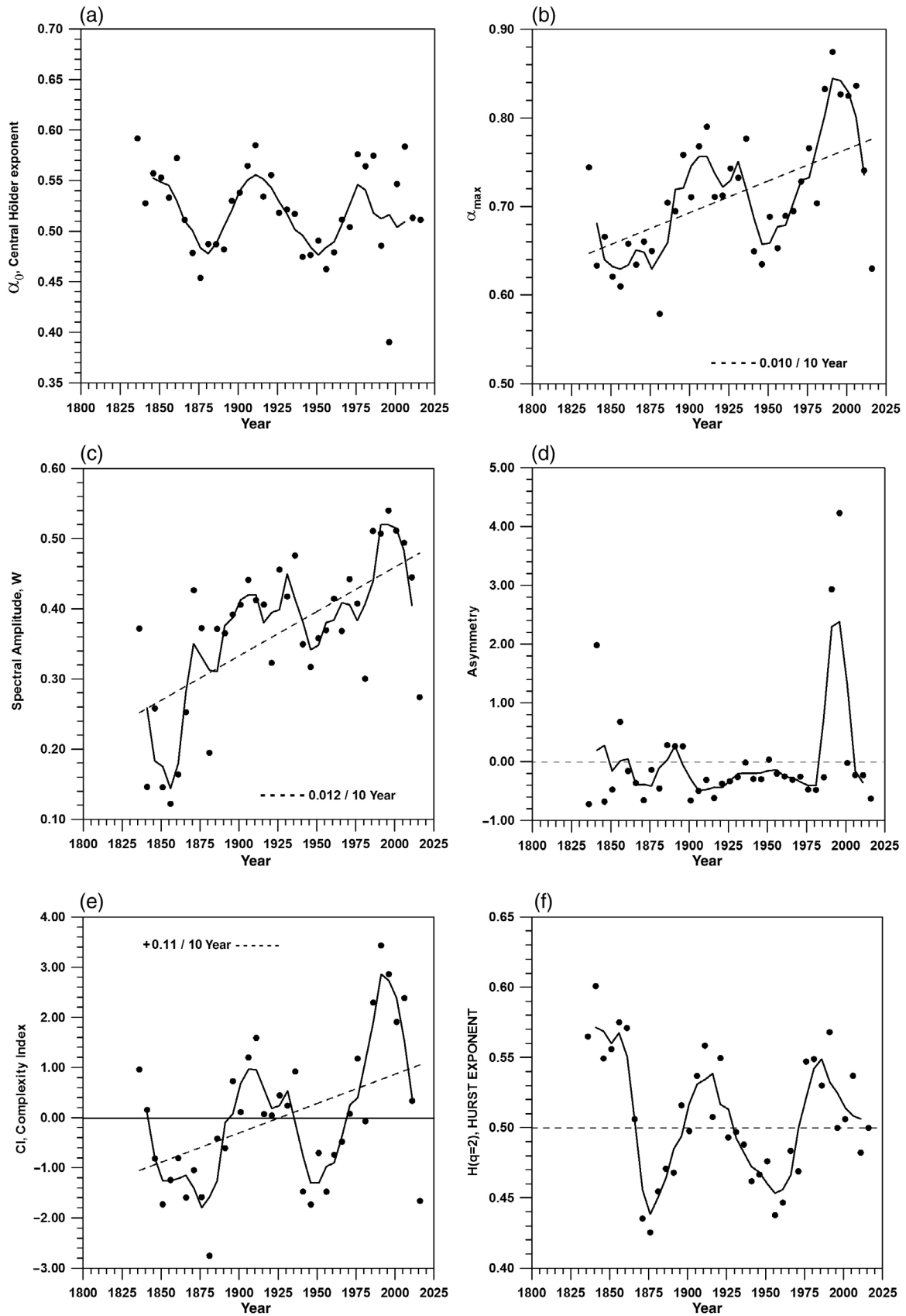


FIGURE 8 Evolution with the moving windows of (a) the central Hölder exponent, α_0 , (b) the maximum Hölder exponent, α_{max} , (c) the spectral amplitude, W , (d) the asymmetry, γ , the complexity index, CI, and (e) the Hurst exponent, $H(q = 2)$

together with the relative increase in extreme rainfall, Casas-Castillo *et al.* (2018a) analysed the temporal evolution of the scale parameter β during the 20th century and

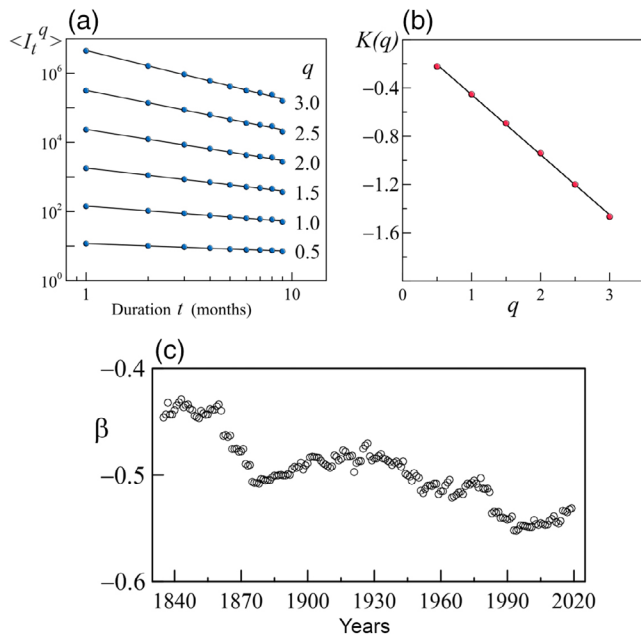


FIGURE 9 (a) Statistical moments for different values of q of the annual maximum intensity. Straight lines indicate scale invariance over a temporal range from 1 to 9 months. (b) Slopes determining the scaling function $K(q)$. (c) Temporal evolution of the scaling parameter β for Barcelona in the scaling regime from 1 to 9 months [Colour figure can be viewed at wileyonlinelibrary.com]

the beginning of the 21th, using sliding intervals of 30 years with 1 year of step. Casas-Castillo *et al.* (2018a) found a slight continuous decrease of the mean value of β for Catalonia (NE of the Iberian Peninsula), indicating a slight progression towards irregularity. At the present work, sliding intervals of 50 years have been used applying the same procedure to detect changes of the scaling behaviour along time, related to changes in rainfall irregularity for the (1840–2019) Barcelona monthly recording period. Figure 9c shows the temporal evolution of β obtained for the monthly series. As it was previously found for Catalonia, the scaling analysis of monthly series for Barcelona indicates a decreasing evolution of the parameter β with values higher than -0.45 since the middle of the 19th century to values around -0.55 at present. This evolution seems to indicate a progression towards irregularity in the monthly series.

Additionally, a detailed revision of Figure 9c depicts four different consecutive tendencies on the scale parameter β since 1830 up to nowadays. The period 1830–1870 is characterized by a clear descending tendency, indicating increasing irregularity on rain amounts for successive months. This tendency is interrupted for the period 1870–1930, being observed a decrease of the irregularity. Nevertheless, for the period 1930–1990 the parameter β notably decreases again, corresponding to years of notable irregularity. Finally, since the last years of the 20th century up to nowadays, new signs of small decreasing irregularity are detected. As a global point of view, the period 1830–2019 is characterized by a reduction close to

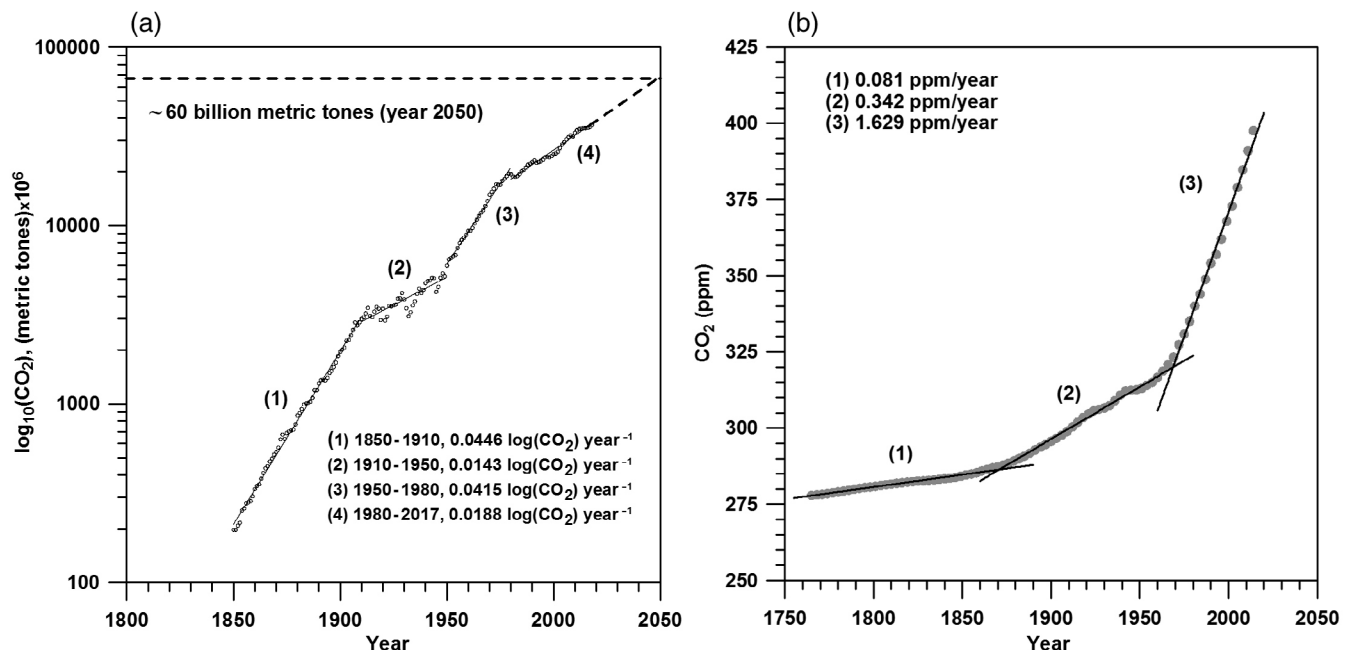


FIGURE 10 (a) Evolution at annual scale of CO_2 emission in the atmosphere, 1850–2018 (data obtained from <https://www.statista.com>, Hamburg, Germany). (b) Evolution at annual scale of tropospheric concentration of CO_2 (Meinshausen *et al.*, 2017)

0.15 units on the β scale parameter, manifesting a statistically significant tendency close to $-0.06/100$ years, incrementing the irregularity on the monthly and annual rainfall regimes.

The evolution of CO_2 emissions to the atmosphere, as well as troposphere concentration (Figure 10a,b), with

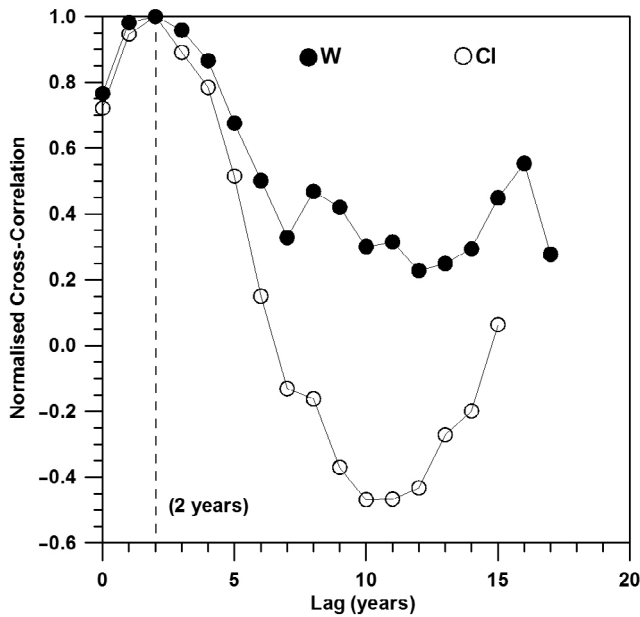


FIGURE 11 Normalized cross-correlation of annual atmospheric concentration of CO_2 and spectral amplitude, W , and complexity index, CI

four intervals of different increases, could be correlated with relevant properties of the analysed pluviometric regime. On the one hand, the global increase on the rainfall amounts fractal irregularity; on the other hand, the increase on the complexity of the multifractal monthly amounts structure and signs of future tendency to monthly amounts randomness. Given that the Pearson coefficient for a possible relationship between rainfall amounts and CO_2 increase is notably small (0.116), this direct dependence on this greenhouse gas becomes very doubtful. Nevertheless, changes on atmospheric CO_2 could condition several pluviometric characteristics (fractal irregularity, complexity and randomness), with a delay for the cross-correlation between annual rainfall and CO_2 increases. The persistence, randomness and anti-persistence, quantified by the Hurst exponent, should not be affected by the CO_2 , given that the corresponding Pearson coefficient is notably small (0.015). Consequently, the oscillations of the Hurst exponent should be attributable to the complexity of the atmospheric physics mechanism. A quite similar small magnitude (-0.022) of the Pearson coefficient is obtained for the central Hölder exponent. Nevertheless, the relationship of multifractal parameters α_{\max} and W with CO_2 increases to 0.499 and 0.463, respectively. Given that these two parameters contribute to CI , a relatively high Pearson coefficient of 0.884 is finally obtained for the pair (CI , CO_2) and the increase of CO_2 could generate a more complex evolution of rainfall amounts. Figure 11

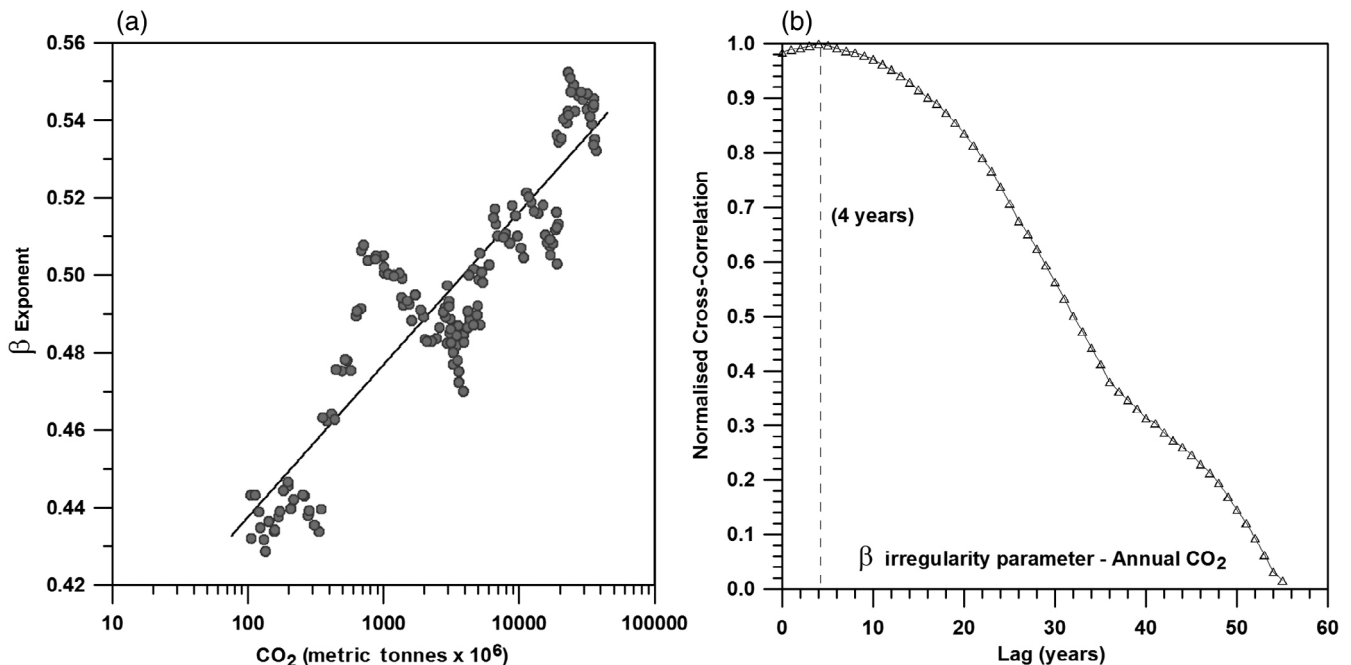


FIGURE 12 Dependence of parameter β on CO_2 , years 1832–2019. (a) Evolution of $|\beta|$ with increasing CO_2 . (b) Cross-correlation between β and CO_2 annual atmospheric concentration

illustrates the cross-correlation between tropospheric CO₂ and spectral amplitudes, W , and complexity indices, CI. In both cases, a delay of 2 years is detected between CO₂ and the two multifractal parameters. These possible correlations between increasing CO₂ and fractal characteristics of the rainfall amounts could be also illustrated by the evolution of the irregularity parameter β , with a global negative tendency towards the extreme irregularity (Figure 9c), characterized by $\beta = -1.0$. The Pearson coefficient achieves a high value, 0.801, suggesting a notable relationship between increases of CO₂ into the atmosphere and more irregularity of the rainfall amount. Figure 12a depicts the possible relationship between β and increasing emissions of CO₂, being quite evident the role of the CO₂ on the irregularity degree of the rainfall series. This evolution is also verified by Figure 12b, depicting the cross-correlation between β and CO₂, characterized by a lag of 4 years, a bit more long than the lag detected for fractal parameters W and CI.

In short, whereas increases on CO₂ emissions into the atmosphere could be related to the increase the complexity and irregularity of the rainfall multifractal structure, oscillations detected on several fractal/multifractal parameters would be only consequence of the physics atmospheric structure. Besides the discarded relationship among monthly, seasonal and annual positive rainfall trends and CO₂ increase, due to the low Pearson coefficient obtained, global positive trends on rainfall amount at annual, seasonal and monthly scales would be contradictory with respect to the expected evolution of the western Mediterranean rainfall regime (Pérez and Boscolo, 2010; Miranda *et al.*, 2011), characterized by reduction of rainfall amounts at monthly and annual scales and by an increase of intense rainfall episodes of short duration. Time trends analysed at seasonal and annual scale for (1950–2019) interval years (Table 2) would confirm, with a clear predominance of negative time trends, a nowadays active reduction on rainfall amounts, except for winter season. It is also worth mentioning that the second expected characteristic of the pluviometric regime in the Western Mediterranean (intense rainfall episodes of short duration) would be in agreement, from the viewpoint of fractal self-similarity and multifractal theory, with increases of irregularity and complexity.

6 | DISCUSSION

The analysis of the pluviometric regime, at monthly, seasonal and annual scales, confirms the expected periodicity, close to 11 years, associated with well established dominant periodical changes on solar radiation. It should

be also cited that the empiric cumulated distribution function of rainfall amounts at seasonal scale is well represented by a single function, the Gumbel distribution, with different parameters for every season. Conversely, although the L -moments procedure suggests the same distribution for the annual series, the discrepancies between theoretical and empirical cumulated distribution functions are quite notable for annual amounts ranging from 200 up to 500–600 mm·year⁻¹.

Based on the Mann–Kendall test, statistical significant time trends are detected at monthly (February, August and September), seasonal (winter and autumn) and annual scales by considering the whole recording period. It is also relevant that, whatever the statistical significance level for every month, most of time trends are positive for the whole recording period at seasonal and annual scale. Nevertheless, the predominant tendency at these scales for the years 1900–1950 and 1950–2019 changes to negative, except for winter. This fact could be partially explained taking into account the last decades of the Little Ice Age (Mann, 2003, among others) for years 1800–1850, and a tendency to recover higher temperatures (years 1850–1900). It is very suggestive the simultaneity of this recovery with the continuous increase of CO₂ emissions along the 20th century and beginning of the 21th, with the subsequent increasing concentration in the troposphere. The results obtained by Serrano-Notivoli *et al.* (2018), who detected a decrease of the frequency of low precipitation events, an increase of the frequency of high and very high events and a significant negative trend in mean amounts when considering all the precipitation days, especially for the Mediterranean coast, would be in agreement with the predominant negative time trends obtained in this research for 1900–1950 and 1950–2019, only departing of this pattern the winter season, and the increase of the fractal irregularity and multifractal complexity. It is also relevant to remember that Fernández-Montes *et al.* (2013) deduced that a great amount of precipitation in the Iberian Peninsula tend to concentrate in relatively few days, primarily conditioned by the atmospheric circulation and the moisture content. These results would be also in agreement with the manifested fractal irregularity increment of the rainfall regime in Barcelona.

Some analyses of rainfall annual trends at European and Mediterranean scales are also relevant, being notably coincident with the results obtained for the Barcelona series analysed in this paper. First of all, Schönwiese and Rapp (1997) detected positive time trends for northern Europe and negative ones for southern Europe. A more detailed annual time trends for the Mediterranean area has been more recently published by Philandras *et al.* (2011). These authors detected 36 annual rainfall series

(years 1900–2010) with negative time trends (20 of them exceeding or equalling 95% statistical certainty and only 9 positive annual series). Additionally, detailing the obtained data on three domains (Western, Central and Eastern Mediterranean), these authors assigned three distinct global negative annual time trends, all of them statistically significant at 95%, corresponding to the Eastern Mediterranean ($-1.50 \text{ mm}\cdot\text{year}^{-1}$), the Central Mediterranean ($-3.01 \text{ mm}\cdot\text{year}^{-1}$) and the Western Mediterranean, the most affected for the climatic change ($-3.61 \text{ mm}\cdot\text{year}^{-1}$). In consequence, at least from the point of view of annual rainfall amounts, Barcelona city and its metropolitan area (Western Mediterranean) would be characterized by one of the most notably affected by the climatic change, with $-1.39 \text{ mm}\cdot\text{year}^{-1}$ trend (90% significant) for years 1900–1950 and $-0.17 \text{ mm}\cdot\text{year}^{-1}$ for 1950–2019.

Given that the time trend signs for the successive 50 years segments and CO_2 increases, the possibility of the rainfall regime being affected by CO_2 emissions and concentration on the troposphere has been analysed by comparing them with self-similarity and fractal and multifractal results, being finally assumed that these emissions could be associated with increasing complexity and irregularity of the rainfall regime, in agreement with the Pearson coefficients obtained, some of them moderate or notably high for pairs of fractal/multifractal parameters and CO_2 concentration. The results of the same strategy, applied to rainfall amounts, are doubtful given that the Pearson coefficients obtained were notably small and a clear relationship between rainfall amount changes and CO_2 increase is not so evident. Nevertheless, the tendency to reduce seasonal and annual amounts along the last 70 years (1950–2019) is quite evident, coincident with a high increase on CO_2 emissions (1950–1980) and years of relatively minor emissions rate (1980–2017), but with continued increments of CO_2 concentration into the atmosphere, varying from 312.8 ppm, year 1950, to 397.5 ppm, year 2017 (Meinshausen *et al.*, 2017). In agreement with Richardson *et al.* (2016), bearing in mind that the changes on rainfall amounts would not be directly affected by the CO_2 evolution, but more depending on the warming of land's surface due to CO_2 emissions, some relationships (in terms of Pearson coefficients for instance) between these tropospheric concentration and changes on rainfall regimes would be difficult to obtain. Consequently, the interpretation of the rainfall amount changes in terms of CO_2 evolution would be another quite different objective for future analyses, always taking into account the mentioned warming of land's surface. Nevertheless, in spite of these mentioned shortcomings, two examples of the possible effects of CO_2 on rainfall characteristics, assuming effects, could be cited. Bütgen *et al.* (2021) have recently analysed, at European scale, the relationship of drought

severity, rainfall irregularity and negative time trends and CO_2 evolution in the atmosphere. At local scale (NE Spain), Lana *et al.* (2021b) have researched the possible dependence of rainfall time trends on CO_2 emissions and tropospheric concentration changes.

With respect to possible monthly rainfall forecasting, the fractal/multifractal parameters, based on self-similarity scaling, the reconstruction theorem and the MDFA algorithm, could suggest a notable complexity on the autoregressive forecasting of monthly amounts. Nevertheless, this shortcoming does not necessarily represent a wrong estimation of forthcoming monthly amounts. The results obtained by Lana *et al.* (2021a), corresponding to the fractal/multifractal theory and the autoregressive ARIMA algorithm applied to forecast monthly rainfall amounts in Catalonia (NE Spain), depicted reasonable small discrepancies between real and forecasting monthly amounts. Taking into account that the database was notably shorter (50–60 years) in comparison with the rainfall series analysed in this research, and that windows lengths less than 300 months were necessary for the successful application of the ARIMA algorithm, forecasting of monthly amounts in Barcelona city could be computed with the nowadays longer monthly series, with a certain degree of confidence. Small forecasting errors would be expected and the necessary number of monthly data to correctly apply the ARIMA algorithm would be absolutely available considering the long data series.

In short, according all these results, the future pluviometric regime in Barcelona city would be characterized, by moderate, but statistically significant, time trends (negatives in agreement with the last 70 years, perhaps with the exception of the winter season) and a gradual and significant increase on the monthly irregularity and complexity (verified by self-similarity and multifractal analyses), being the increment on the CO_2 emissions a possible correlation factor of this evolution, a question to be investigated with more detail in future researches. It is also noticeable that these results obtained for Barcelona city could be also useful to prevent the effects of future changes on rainfall patterns affecting other cities of the same metropolitan area, close each other, all of them emplaced along a continuous urbanized narrow fringe delimited by the Western Mediterranean coast and the Littoral and Pre-Littoral chains, and with a dense population exceeding 3.5 million inhabitants.

7 | CONCLUSIONS

The long rainfall records, at monthly and annual scales, in Barcelona city have permitted detailed analyses of the rainfall patterns since years 1786 up to 2019. Periodicity at annual scale, time trends of complete series and

50 years segments, with the corresponding results of statistical significance, based on the Mann–Kendall test, have permitted to obtain a first point of view of the rainfall amounts evolution. The different year intervals could be assumed coincident with the last period of the Little Ice Age, the recovery of temperature levels and, finally, with the high increases of CO₂ emissions and concentrations in the troposphere along the 20th century and the beginning of the 21st century.

In spite of the relationship between rainfall amounts and CO₂ emissions, as well as tropospheric concentration, have been discarded due to small Pearson coefficients and the necessity of land's warming data for a better interpretation, the effects of CO₂ have been better detected (again by means of Pearson coefficient values) by mean of the parameters of the multifractal analysis and self-similarity scaling results, with evidences of increasing structural complexity and irregularity of rainfall series, associated with increasing CO₂ emissions and their concentration in the troposphere.

Finally, this possible rainfall patterns–CO₂ correlation is expected to be complemented by taking advantage of warming land's surface data, probably much more depending on GHGs (greenhouse gasses) increments than some patterns of the pluviometric regimes.

AUTHOR CONTRIBUTIONS

Conceptualisation: Xavier Lana, Raül Rodríguez-Solà and M. Carmen Casas-Castillo. **Methodology:** Xavier Lana, Raül Rodríguez-Solà and M. Carmen Casas-Castillo. **Software:** Xavier Lana, Raül Rodríguez-Solà and Ricard Kirchner. **Validation:** Xavier Lana, M. Carmen Casas-Castillo, Raül Rodríguez-Solà and Marc Prohom. **Formal analysis:** Xavier Lana, Raül Rodríguez-Solà and M. Carmen Casas-Castillo. **Investigation:** Xavier Lana. **Resources:** Xavier Lana and Marc Prohom. **Data curation:** Xavier Lana and Marc Prohom. **Writing – original draft preparation:** Xavier Lana and M. Carmen Casas-Castillo. **Writing – review and editing:** Xavier Lana, M. Carmen Casas-Castillo, Raül Rodríguez-Solà, Carina Serra and Maria Dolors Martínez. **Figures and visualization:** Xavier Lana, M. Carmen Casas-Castillo and Raül Rodríguez-Solà. **Supervision:** Xavier Lana, M. Carmen Casas-Castillo, Raül Rodríguez-Solà and Marc Prohom. **Funding acquisition:** Xavier Lana, Carina Serra and Maria Dolors Martínez. All authors have read and agreed to the published version of the manuscript.

ACKNOWLEDGEMENTS

This research was supported by the Spanish Ministry of Science, Innovation and Universities (Grant No. PID2019-105976RB-I00) and (Grant No. AGL2017-87658-R).

CONFLICT OF INTEREST

The authors declare no potential conflict of interest.

ORCID

Xavier Lana  <https://orcid.org/0000-0002-3298-9234>

M. Carmen Casas-Castillo  <https://orcid.org/0000-0002-7507-6195>

Raül Rodríguez-Solà  <https://orcid.org/0000-0002-9623-894X>

REFERENCES

- Aldrian, E. and Djamil, Y.S. (2007) Spatial-temporal climatic change of rainfall in East Java Indonesia. *International Journal of Climatology*, 28, 435–438.
- Arnbjerg-Nielsen, K., Willems, P., Olsson, J., Beecham, S., Pathirana, A., Bülow Gregersen, I., Madsen, H. and Nguyen, V. T.V. (2013) Impacts of climate change on rainfall extremes and urban drainage systems: a review. *Water Science and Technology*, 68, 16–28.
- Bara, M., Gaál, L., Kohnová, S., Szolgay, J. and Hlavčová, K. (2010) On the use of the simple scaling of heavy rainfall in a regional estimation of IDF curves in Slovakia. *Journal of Hydrology and Hydromechanics*, 58(1), 49–63. <https://doi.org/10.2478/v10098-010-0006-0>.
- Burgueño, A., Codina, B., Redaño, A. and Lorente, J. (1994) Basic statistical characteristics of hourly rainfall amounts in Barcelona. *Theoretical and Applied Climatology*, 49, 175–181. <https://doi.org/10.1007/BF00865532>.
- Burgueño, A., Lana, X., Serra, C. and Martínez, M.D. (2014) Daily extreme temperature multifractals in Catalonia (NE Spain). *Physical Letters A*, 378, 874–885.
- Burgueño, A., Martínez, M.D., Lana, X. and Serra, C. (2005) Statistical distributions of the daily rainfall regime in Catalonia (NE Spain) for the years 1950–2000. *International Journal of Climatology*, 25, 1381–1403.
- Burgueño, A., Serra, C. and Lana, X. (2004) Monthly and annual statistical distributions of the daily rainfall at the Fabra Observatory (Barcelona, NE Spain) for the years 1917–1999. *Theoretical and Applied Climatology*, 77, 57–75.
- Burlando, P. and Rosso, R. (1996) Scaling and multiscaling models of depth-duration-frequency curves for storm precipitation. *Journal of Hydrology*, 187, 45–64. [https://doi.org/10.1016/S0022-1694\(96\)03086-7](https://doi.org/10.1016/S0022-1694(96)03086-7).
- Bütgen, U., Urban, O., Krusic, P.J., Rybniček, M., Kolař, T., Kyncl, T., Ač, A., Koňasova, E., Časlavský, J., Esper, J., Wagner, S., Saurer, M., Tegel, W., Dobrovolný, P., Cherubini, P., Reinig, F. and Trnka, M. (2021) Recent European drought extremes beyond Common Era background variability. *Nature Geoscience*, 14, 190–196. <https://doi.org/10.1038/s41561-021-00698-0>.
- Cameron, R.H. and Schüssler, M. (2019) Solar activity: periodicities beyond 11 years are consistent with random forcing. *Astronomy and Astrophysics*, 625, A28. <https://doi.org/10.1051/0004-6361/201935290>.
- Casas, M.C., Codina, B., Redaño, A. and Lorente, J. (2004) A methodology to classify extreme rainfall events in the western Mediterranean area. *Theoretical and Applied Climatology*, 77, 139–150. <https://doi.org/10.1007/s00704-003-0003-x>.

- Casas, M.C., Rodríguez, R. and Redaño, Á. (2010) Analysis of extreme rainfall in Barcelona using a microscale rain gauge network. *Meteorological Applications*, 17, 117–123. <https://doi.org/10.1002/met.166>.
- Casas-Castillo, M.C., Llabrés-Brustenga, A., Rius, A., Rodríguez-Solà, R. and Navarro, X. (2018a) A single scale parameter as a first approximation to describe the rainfall pattern of a place: application on Catalonia. *Acta Geophysica*, 66(3), 415–425. <https://doi.org/10.1007/s11600-018-0122-5>.
- Casas-Castillo, M.C., Rodríguez-Solà, R., Llabrés-Brustenga, A., García-Marín, A.P., Estévez, J. and Navarro, X. (2022) A simple scaling analysis of rainfall in Andalusia (Spain) under different precipitation regimes. *Water*, 14, 1303. <https://doi.org/10.3390/w14081303>.
- Casas-Castillo, M.C., Rodríguez-Solà, R., Navarro, X., Russo, B., Lastra, A., González, P. and Redaño, Á. (2018b) On the consideration of scaling properties of extreme rainfall in Madrid (Spain) for developing a generalized intensity-duration-frequency equation and assessing probable maximum precipitation estimates. *Theoretical and Applied Climatology*, 131(1–2), 573–580. <https://doi.org/10.1007/s00704-016-1998-0>.
- Christensen, J.H. and Christensen, O.B. (2003) Severe summertime flooding in Europe. *Nature*, 421, 805–806. <https://doi.org/10.1038/421805a>.
- De Lima, M.I.P. and De Lima, J.L.M.P. (2009) Investigating the multifractality of point precipitation in the Madeira archipelago. *Nonlinear Processes in Geophysics*, 16, 299–311. <https://doi.org/10.5194/npg-16-299-2009>.
- De Lima, M.I.P. and Grasman, J. (1999) Multifractal analysis of 15-min and daily rainfall from a semi-arid region in Portugal. *Journal of Hydrology*, 220(1–2), 1–11. [https://doi.org/10.1016/S0022-1694\(99\)00053-0](https://doi.org/10.1016/S0022-1694(99)00053-0).
- Diks, C. (1999) Nonlinear time series analysis. Methods and applications. In: Tong, H. (Ed.) *Nonlinear Time Series and Chaos*, Vol. 4. London: World Scientific, 209 pp.
- Eckmann, J.P., Oliffson, S., Ruelle, D. and Ciliberto, S. (1986) Lyapunov exponents from time series. *Physical Review A*, 34, 4971–4979.
- Estévez, J., Llabrés-Brustenga, A., Casas-Castillo, M.C., García-Marín, A.P., Kirchner, R. and Rodríguez-Solà, R. (2022) A quality control procedure for long-term series of daily precipitation data in a semiarid environment. *Theoretical and Applied Climatology*. <https://doi.org/10.1007/s00704-022-04089-2>.
- Fernández-Montes, S., Seubert, S., Rodrigo, F.S., Rasilla Álvarez, D. F., Hertig, E., Esteban, P. and Philipp, A. (2013) Circulation types and extreme precipitation days in the Iberian Peninsula in the transition seasons: spatial links and temporal changes. *Atmospheric Research*, 138, 41–58. <https://doi.org/10.1016/j.atmosres.2013.10.018>.
- Fraedrich, K. and Larnder, C. (1993) Scaling regimes of composite rainfall time series. *Tellus A*, 45(4), 289–298. <https://doi.org/10.3402/tellusa.v45i4.14893>.
- García-Marín, A.P., Ayuso-Muñoz, J.L., Jiménez-Hornero, F.J. and Estévez, J. (2013) Selecting the best IDF model by using the multifractal approach. *Hydrological Processes*, 27, 433–443. <https://doi.org/10.1002/hyp.9272>.
- Goltz, C. (1997) Fractal and chaotic properties of earthquakes. In: *Lecture Notes in Earth Sciences*, Vol. 77. Berlin: Springer, 178 pp.
- Grassberger, P. and Procaccia, I. (1983a) Characterization of strange attractors. *Physical Review Letters*, 50, 346–349.
- Grassberger, P. and Procaccia, I. (1983b) Estimation of the Kolmogorov entropy from a chaotic signal. *Physics Review A*, 28, 448–451.
- Gupta, V.K. and Waymire, E. (1990) Multiscaling properties of spatial and river flow distributions. *Journal of Geophysical Research*, 95(D3), 1999–2009. <https://doi.org/10.1029/JD095iD03p01999>.
- Hosking, J.R.M. and Wallis, J.R. (1997) *Regional Frequency Analysis. An Approach Based on L-Moments*. Cambridge: Cambridge University Press, 224 pp.
- Kantelhardt, J.W., Zschiegner, S.A., Koscielny-Bunde, A., Havlin, S., Bunde, A. and Stanley, H.E. (2002) Multifractal detrended fluctuation analysis of nonstationary time series. *Physica A: Statistical Mechanics and its Applications*, 316, 87–114.
- Kaplan, J.K. and Yorke, J.A. (1979) Chaotic behaviour of multidimensional difference equations. In: Walter, H.O. and Peitgen, H.O. (Eds.) *Functional Difference Equations and Approximation of Fixed Points*, Vol. 730. Berlin: Springer, pp. 204–227.
- Korvin, G. (1992) *Fractal Models in the Earth Sciences*. Amsterdam: Elsevier, 396 pp.
- Koutsoyiannis, D. and Foufoula-Georgiou, E. (1993) A scaling model of storm hyetograph. *Water Resources Research*, 29(7), 2345–2361. <https://doi.org/10.1029/93WR00395>.
- Ladou, P., Schmitt, F., Schertzer, D. and Lovejoy, S. (1993) Variabilité temporelle des observations pluviométriques à Nîmes. *Comptes Rendus de l'Académie des Sciences*, 317, 775–782.
- Lana, X., Burgueño, A., Serra, C. and Martínez, M.D. (2017) Monthly rain amounts at Fabra Observatory (Barcelona, NE Spain): fractal structure, autoregressive processes and correlation with monthly Western Mediterranean oscillation index. *International Journal of Climatology*, 37, 1557–1577. <https://doi.org/10.1002/joc.4797>.
- Lana, X., Casas-Castillo, M.C., Rodríguez-Solà, R., Serra, C., Martínez, M.D. and Kirchner, R. (2021b) Rainfall regime trends at annual and monthly scales in Catalonia (NE Spain) and indications of CO₂ emissions effects. *Theoretical and Applied Climatology*, 146, 981–996. <https://doi.org/10.1007/s00704-021-03773-z>.
- Lana, X., Casas-Castillo, M.C., Serra, C., Rodríguez-Solà, R., Redaño, Á., Burgueño, A. and Martínez, M.D. (2019) Return period curves for extreme 5-min rainfall amounts at the Barcelona urban network. *Theoretical and Applied Climatology*, 135, 1243–1257. <https://doi.org/10.1007/s00704-018-2434-4>.
- Lana, X., Rodríguez-Solà, R., Martínez, M.D., Casas-Castillo, M.C., Serra, C. and Burgueño, A. (2020b) Characterization of standardized heavy rainfall profiles for Barcelona city: clustering, rain amounts and intensity peaks. *Theoretical and Applied Climatology*, 142, 255–268. <https://doi.org/10.1007/s00704-020-03315-z>.
- Lana, X., Rodríguez-Solà, R., Martínez, M.D., Casas-Castillo, M.C., Serra, C. and Kirchner, R. (2021a) Autoregressive process of monthly rainfall amounts in Catalonia (NE Spain) and improvements on predictability of length and intensity of drought episodes. *International Journal of Climatology*, 41, 3178–3194. <https://doi.org/10.1002/joc.6915>.

- Lana, X., Rodríguez-Solà, R., Martínez, M.D., Casas-Castillo, M.C., Serra, C. and Kirchner, R. (2020a) Multifractal structure of the monthly rainfall regime in Catalonia (NE Spain): evaluation of the non-linear structural complexity of the monthly rainfall. CHAOS: interdisciplinary. *Journal of Nonlinear Science*, 30(7), 073117. <https://doi.org/10.1063/5.0010342>.
- Lana, X., Serra, C. and Burgueño, A. (2001) Patterns of monthly rainfall shortage and excess in terms of the standardized precipitation index for Catalonia (NE Spain). *International Journal of Climatology*, 21, 1669–1691.
- Lana, X., Serra, C. and Burgueño, A. (2003) Trends affecting pluviometric indices at the Fabra Observatory (Barcelona, NE Spain) from 1917 to 1999. *International Journal of Climatology*, 23, 315–332.
- Liuzzo, L. and Freni, G. (2015) Analysis of extreme rainfall trends in sicily for the evaluation of depth–duration–frequency curves in climate change scenarios. *Journal of Hydrological Engineering*, 20(12), 04015036.
- Mann, M. (2003) Little ice age ice. In: MacCracken, M.C. and Perry, J. S. (Eds.) *Encyclopedia of Global Environmental Change. The Earth System: Physical and Chemical Dimensions of Global Environmental Change*, Vol. 1. Chichester, UK: John Wiley & Sons.
- Mansell, M.G. (1997) The effect of climate change on rainfall trends and flooding risk in the west of Scotland. *Hydrology Research*, 28(1), 37–50.
- Martínez, M.D., Lana, X., Burgueño, A. and Serra, C. (2007) Spatial and temporal daily rainfall regime in Catalonia (NE Spain) derived from four precipitation indices, years 1950–2000. *International Journal of Climatology*, 27, 123–138.
- Martín-Vide, J. and Moreno-García, M.C. (2021) Análisis de la serie secular de precipitación anual del Observatorio Fabra (Barcelona) (1914–2020). *Geographica*, 73, 81–94. https://doi.org/10.26754/ojs_geoph/geoph.2021735192.
- Meinshausen, M., Vogel, E., Nauels, A., Lorbacher, K., Meinshausen, N., Etheridge, D.M., Fraser, P.J., Montzka, S.A., Rayner, P.J., Trudinger, C.M., Krummel, P.B., Beyerle, U., Canadell, J.G., Daniel, J.S., Enting, I.J., Law, R.M., Lunder, C. R., O'Doherty, S., Prinn, R.G., Reimann, S., Rubino, M., Velders, G.J.M., Vollmer, M.K., Wang, R.H.J. and Weiss, R. (2017) Historical greenhouse gas concentrations for climate modelling (CMIP6). *Geoscientific Model Development*, 10, 2057–2116. <https://doi.org/10.5194/gmd-10-2057-2017>.
- Menabde, M., Seed, A. and Pegram, G. (1999) A simple scaling model for extreme rainfall. *Water Resources Research*, 35(1), 335–339. <https://doi.org/10.1029/1998WR900012>.
- Miranda, J.D., Armas, C., Padilla, F.M. and Pugnaire, F.I. (2011) Climatic change and rainfall patterns: effects on semi-arid plant communities of the Iberian southeast. *Journal of Arid Environments*, 75, 1302–1309.
- Mirhosseini, G., Srivastava, P. and Stefanova, L. (2013) The impact of climate change on rainfall intensity–duration–frequency (IDF) curves in Alabama, USA. *Regional Environment Change*, 13, 25–33.
- Murphy, C., Broderick, C., Burt, T. P., Curley, M., Duffy, C., Hall, J., Harrigan, S., Matthews, T. K. R., Macdonald, N., McCarthy, G., McCarthy, M. P., Mullan, D., Noone, S., Osborn, T. J., Ryan, C., Sweeney, J., Thorne, P. W., Walsh, S., and Wilby, R. L., 2018. A 305-year continuous monthly rainfall series for the Island of Ireland (1711–2016). *Climate of the Past* 14, 413–440, <https://doi.org/10.5194/cp-14-413-2018>, 2018, 440.
- Nhat, L.M., Tachikawa, Y., Sayama, T. and Takara, K. (2007) Regional rainfall intensity–duration–frequency relationships for ungauged catchments based on scaling properties. *Annual Report of Disaster Prevention Research Institute, Kyoto University*, 50, 33–43.
- Olsson, J. (1995) Limits and characteristics of the multifractal behaviour of a high-resolution rainfall time series. *Nonlinear Processes in Geophysics*, 2(1), 23–29. <https://doi.org/10.5194/npg-2-23-1995>.
- Pérez, F. F. and Boscolo, R. (2010) *Clima en España: Pasado, presente y futuro. Informe de Evaluación del Cambio climático Regional. Red Temática CLIVAR-España*. Spanish: Ministry of Science and Innovation and Ministry of Environment. Available at: http://clivar.iim.csic.es/files/informe_clivar_final.pdf.
- Philandras, C.M., Nastos, P.T., Kapsomenakis, J., Douvis, K.C., Selioudis, G.T. and Zerefos, C.S. (2011) Long term precipitation trends and variability within the Mediterranean region. *Natural Hazards and Earth System Sciences*, 11, 3235–3250.
- Prohom, M., Barriendos, M. and Sánchez-Lorenzo, A. (2015) Reconstruction and homogenization of the longest instrumental precipitation series in the Iberian Peninsula (Barcelona, 1786–2014). *International Journal of Climatology*, 36(8), 3072–3087. <https://doi.org/10.1002/joc.4537>.
- Richardson, T.B., Foster, P.M., Andrews, T. and Parker, D.J. (2016) Understanding the rapid precipitation response to CO₂ and aerosol forcing on a regional scale. *Journal of Climate*, 29, 583–594. <https://doi.org/10.1175/JCLI-D-15-0174.1>.
- Rodríguez, R., Casas, M.C. and Redaño, Á. (2013a) Multifractal analysis of the rainfall time distribution on the metropolitan area of Barcelona (Spain). *Meteorology and Atmospheric Physics*, 121(3–4), 181–187. <https://doi.org/10.1007/s00703-013-0256-6>.
- Rodríguez, R., Navarro, X., Casas, M.C. and Redaño, Á. (2013b) Rainfall spatial organization and areal reduction factors in the metropolitan area of Barcelona (Spain). *Theoretical and Applied Climatology*, 114, 1–8. <https://doi.org/10.1007/s00704-012-0818-4>.
- Rodríguez, R., Navarro, X., Casas, M.C., Ribalaygua, J., Russo, B., Pouget, L. and Redaño, Á. (2014) Influence of climate change on IDF curves for the metropolitan area of Barcelona (Spain). *International Journal of Climatology*, 34, 643–654. <https://doi.org/10.1002/joc.3712>.
- Rodríguez-Solà, R., Casas-Castillo, M.C., Navarro, X. and Redaño, Á. (2017) A study of the scaling properties of rainfall in Spain and its appropriateness to generate intensity–duration–frequency curves from daily records. *International Journal of Climatology*, 37(2), 770–780. <https://doi.org/10.1002/joc.4738>.
- Royer, J.F., Biauou, A., Chauvin, F., Schertzer, D. and Lovejoy, S. (2008) Multifractal analysis of the evolution of simulated precipitation over France in a climate scenario. *Comptes Rendus Geoscience*, 340(7), 431–440. <https://doi.org/10.1016/j.crte.2008.05.002>.
- Schönwiese, C. and Rapp, J. (1997) *Climate Trend Atlas of Europe Based on Observations 1891–1990*. Dordrecht: Kluwer Academic, 224 pp.
- Serrano-Notivol, R., Beguería, S., Saz, M.A. and de Luis, M. (2018) Recent trends reveal decreasing intensity of daily precipitation in Spain. *International Journal of Climatology*, 38, 4211–4224. <https://doi.org/10.1002/joc.5562>.
- Shimizu, Y., Thurner, S. and Ehrenberger, K. (2002) Multifractal spectra as a measure of complexity human posture. *Fractals*, 10, 104–116.

- Stopp, F. and Meier, P.F. (1988) Evaluation of Lyapunov exponents and scaling functions from time series. *Journal of the Optical Society of America B*, 5, 1037–1045.
- Tessier, Y., Lovejoy, S., Hubert, P., Schertzer, D. and Pecknold, S. (1996) Multifractal analysis and modeling of rainfall and river flows and scaling, causal transfer functions. *Journal of Geophysical Research*, 101, 26247–26440. <https://doi.org/10.1029/96JD01799>.
- Turcotte, D.L. (1997) *Fractal and Chaos in Geology and Geophysics*, 2nd edition. Cambridge: Cambridge University Press, p. 398.
- Wiggins, S. (2003) Introduction to applied nonlinear dynamical systems and chaos. In: *Texts in Applied Mathematics*, Vol. 2, 2nd edition. New York, NY: Springer, p. 844.
- Yu, P.S., Yang, T.H. and Lin, C.S. (2004) Regional rainfall intensity formulas based on scaling property rainfall. *Journal of Hydrology*, 29, 108–123. <https://doi.org/10.1016/j.jhydrol.2004.03.003>.
- Zhang, Q., Harman, C.J. and Kirchner, J.W. (2017) Evaluation of statistical methods for quantifying fractal scaling in water quality time series with irregular sampling. *Hydrology and Earth System Sciences Discussions*, 22, 1175–1192. <https://doi.org/10.5194/hess-2017-315>.

How to cite this article: Lana, X., Casas-Castillo, M. C., Rodríguez-Solà, R., Prohom, M., Serra, C., Martínez, M. D., & Kirchner, R. (2022). Time trends, irregularity and multifractal structure on the monthly rainfall regime at Barcelona, NE Spain, years 1786–2019. *International Journal of Climatology*, 1–20. <https://doi.org/10.1002/joc.7786>